CHAPTER

6 Current regulators of alternating current motors

A current regulator plays a role in making a motor current achieve its desired value, and is an essential part of the vector control system for alternating current (AC) motors. For an accurate instantaneous torque control by using the vector control, the actual motor currents must follow the current commands required to produce the flux and torque regardless of hindrances such as back-electromotive force (back-EMF), leakage inductance, and resistance of windings. Thus for the implementation of the vector control system, it is very important to design the current regulator well. In this chapter we will examine the current regulation techniques for the vector control system of AC motors.

The system configuration for the current control of a three-phase load is shown in Fig. 6.1. The current regulator plays a role in generating gating signals for the switching devices of a pulse width modulation (PWM) inverter, which can produce the output voltage to make the required current flow into the three-phase load.

In other words, the main function of the current regulator is to transform the current error into gating signals for the switching devices in the time domain.

For the case of using a voltage source type PWM inverter, there have been four different types of current regulators researched as:

- Predictive current regulator
- Hysteresis current regulator
- Ramp comparison current regulator or sine-triangle comparison regulator
- $d-q$ axes current regulator

A current regulator consists of an error compensation part and a voltage modulation part as shown in Fig. 6.2. The error compensation part produces a command voltage to reduce the error between the actual and command currents, whereas the voltage modulation part generates gating signals for switching devices to accurately produce the command voltage given by the error compensation part.

In the conventional regulators, such as a predictive current regulator, hysteresis current regulator, and ramp comparison current regulator, the error compensation part and the voltage modulation part are formed as one. In contrast, in a $d-q$ axes current regulator, these two parts are constructed separately. In this regulator a proportional integral (PI) controller is commonly used for the error compensation. Various PWM techniques are used for the voltage modulation, which will be described in Chapter 7.

Electric Motor Control. DOI: http://dx.doi.org/10.1016/B978-0-12-812138-2.00006-4

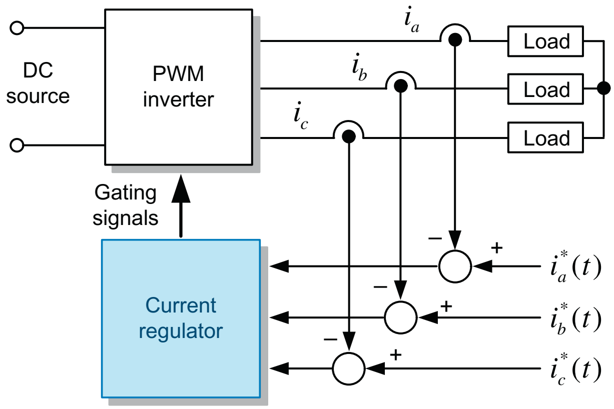

FIGURE 6.1

Current control of a three-phase load.

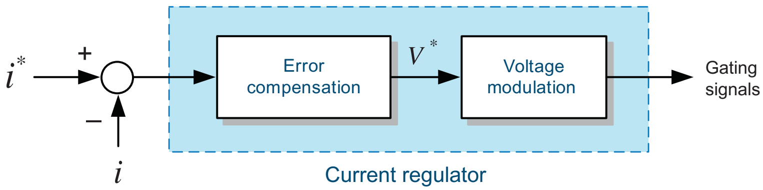

FIGURE 6.2

Configuration of a current regulator.

Now we will explore these current regulators. First, we discuss briefly the predictive current regulator, which is based on a mathematical model of the load. In the predictive current regulator the current error is calculated at every current control period, and the required voltage is determined to minimize the error using the load mathematical model. Afterward, the on/off states of the switching devices are directly chosen to produce the required voltage. The actual load current in the predictive current regulator may lag behind the command current by more than one sampling time. Furthermore, its performance will be greatly affected by the variation of parameters used in the load mathematical model. Next, we will examine the rest of the current regulators in more detail.

6.1 HYSTERESIS REGULATOR

As a type of bang–bang control, a hysteresis regulator is the simplest current controller, directly controlling the on/off states of switches according to the current error. The operation principle of a hysteresis controller is as follows [1].

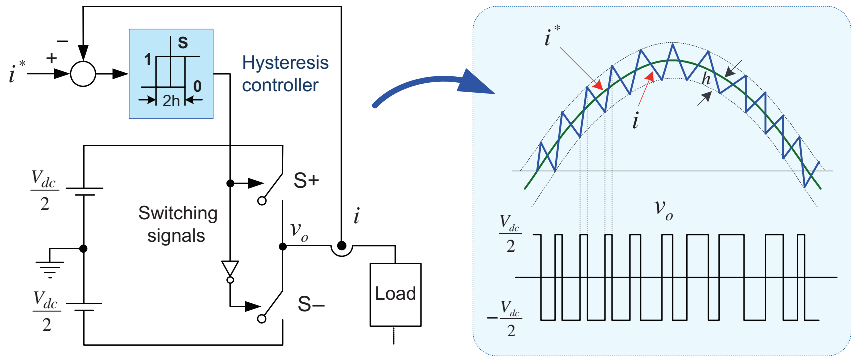

FIGURE 6.3

Operation principle of a hysteresis regulator.

In the hysteresis regulator, as shown in Fig. 6.3, if the error between the actual current and the command current is more than the preset value h (called *hysteresis band*), then the state of the switch is changed to reduce the error. In other words, the state of the switches is changed whether the actual current is greater or less than the command current by the hysteresis band h as:

- $i^* - i \leq -h$: lower switch S− is turned on to decrease the load current by producing a negative voltage $(-\frac{1}{2}V_{dc})$
- $i^* - i \geq h$: upper switch S+ is turned on to increase the load current by producing a positive voltage $(\frac{1}{2}V_{dc})$

Fig. 6.4 describes the operating range of an actual current vector $\mathbf{i}$ in the complex plane for the hysteresis control. For example, if the actual current of the phase a increases more than its command, then the actual current vector $\mathbf{i}$ moves to the positive (+) of the phase a axis. If the current error of the phase a is equal to the hysteresis band $-h$, then the current vector $\mathbf{i}$ reaches the −A line. At this moment, the lower switch (S−) of the phase a will be turned on and the output voltage will become $-V_{dc}/2$. This will cause the current to decrease. On the contrary, if the current error of the phase a becomes h, then the current vector $\mathbf{i}$ reaches the +A line. Thus the upper switch (S+) will be turned on and the output voltage will become $V_{dc}/2$. This will cause the current to increase.

Likewise, for the phases b and c, the switching actions can be done independently with their own hysteresis band. Since the error of each phase current is limited within h by the hysteresis action, the operating area of the current vector $\mathbf{i}$ can be considered to be inside the hexagon consisting of the six switching lines of the three-phase axes. However, in practice, the current errors can vary up to double the hysteresis band, $2h$, for a Y(wye)-connected three-phase load with a floating neutral point. In that load, the sum of the three-phase currents is zero (i.e., $i_{as} + i_{bs} + i_{cs} = 0$), and thus all three-phase currents cannot be controlled independently. This results in the current errors of 2h.

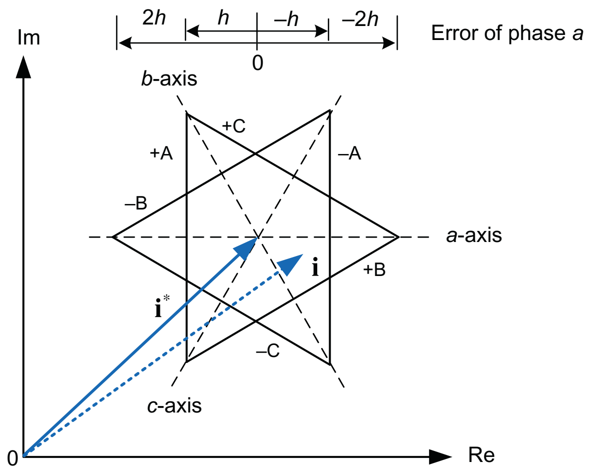

FIGURE 6.4

Operating range of current vector for hysteresis control [1].

Hysteresis current regulators have been widely used for small systems because of their simple implementation and an excellent dynamic performance. However, hysteresis controllers are inherently an analog controller. In addition, the switching frequency is not constant since the turn-on/off instants of switches can change with the back-EMF and load condition. This makes the thermal design of a switching power converter and the filter design of switching noise elimination difficult because the losses and the harmonics generated by the switching actions are a function of the switching frequency. For these reasons, its usage nowadays is limited. In addition, the switching frequency may increase sharply (called *limit cycle*) at low operating frequencies, where only the effective voltage vectors are more likely to be selected due to a small back-EMF. This problem may be improved by adding an offset to the hysteresis band.

6.2 RAMP COMPARISON CURRENT REGULATOR [1]

In a ramp comparison current regulator as shown in Fig. 6.5, the switching states are determined by comparing the current error with the triangular carrier wave based on the following principle:

- Current error $i_{err}>$ carrier wave: upper switch S+ is turned on to produce a positive voltage ($\frac{1}{2}V_{dc}$).
- Current error $i_{err}<$ carrier wave: lower switch S− is turned on to produce a negative voltage ($-\frac{1}{2}V_{dc}$).

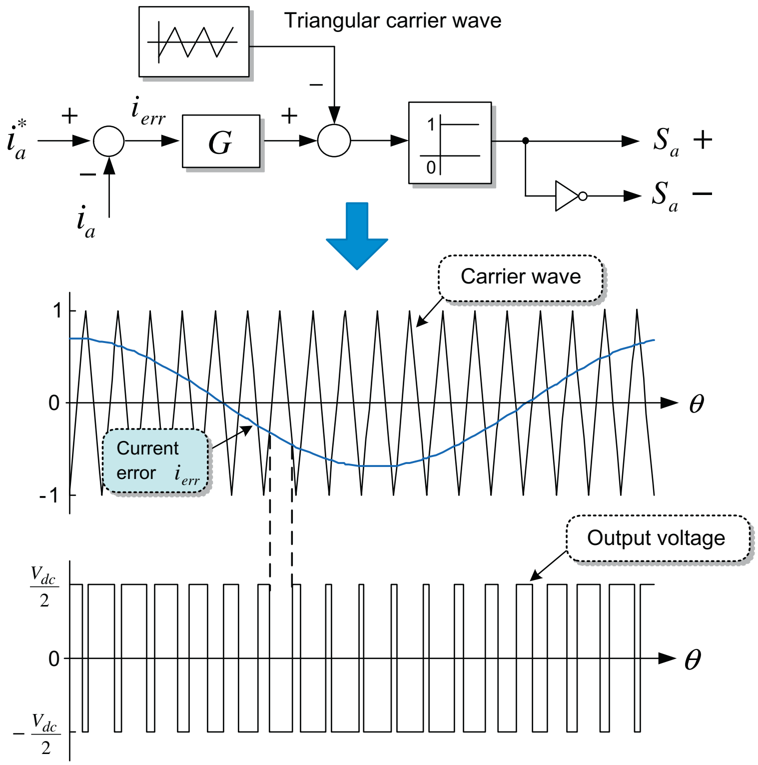

FIGURE 6.5

Operation principle of the ramp comparison current regulator.

For a proper operation of this regulator, the current error should be less than the triangle carrier wave. In this regulator it can be seen that the switching states are changed only at the intersection of the current error and the triangular carrier wave. Thus the switching frequency is equal to the triangle wave frequency and becomes constant. This is a big advantage of this regulator over the hysteresis regulators. However, one major drawback of this regulator is that it has steady-state magnitude and phase errors in the resultant current.

The performance of this regulator is shown in Fig. 6.6. We can see that the actual current has steady-state errors in amplitude and phase with regard to the reference current. These errors increase with the back-EMF, and thus it is hard to obtain a good current regulation performance at high speed operation. A compensator G such as a P (proportional) or PI controller is often used to reduce these errors as shown in Fig. 6.5. Although larger gains can reduce the errors, there is a limit to increasing the gains due to the increase in noise sensitivity. Moreover, a PI controller is unsatisfactory for alternating current (AC) regulation because it can eliminate the control error completely for only direct current (DC) regulation.

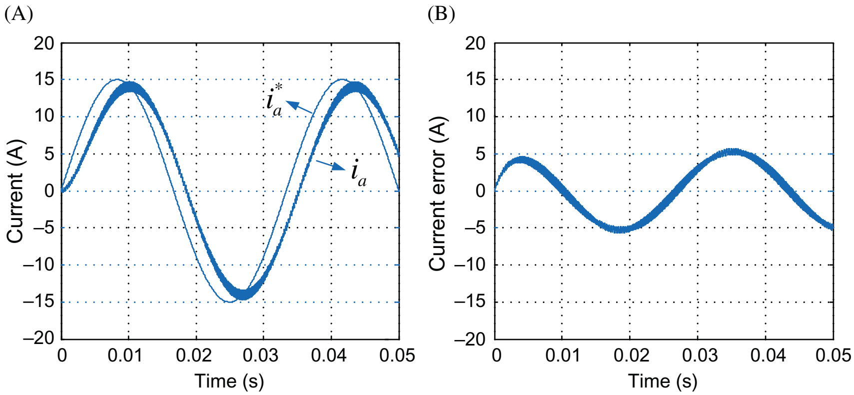

FIGURE 6.6

Performance of the ramp comparison current control. (A) Reference current and actual current and (B) current error.

6.3 *d-q* AXES CURRENT REGULATORS

Since a three-phase AC motor has three stator currents, we may consider at first that three current controllers are needed to regulate their currents individually. However, since their windings are commonly connected in wye with a floating neutral point, the sum of their currents is equal to zero and thus only two of the currents are controllable independently. In addition, the vector control uses the two currents of *d*- and *q*-axes, which the three-phase currents are transformed into. Therefore it is natural to use only two independent current controllers for the control of the three-phase currents of an AC motor.

Now we will introduce the regulator to control the two currents of *d*- and *q*-axes.

6.3.1 STATIONARY REFERENCE FRAME *d-q* CURRENT REGULATOR [2,3]

To begin with, consider the current control for a typical three-phase load as shown in Fig. 6.7. A three-phase load can be generalized as a circuit of $R-L$ and back-EMF and can be expressed as

$$
\begin{aligned}
v_{as} &= Ri_{as} + L\frac{di_{as}}{dt} + e_{as} \\
v_{bs} &= Ri_{bs} + L\frac{di_{bs}}{dt} + e_{bs} \\
v_{cs} &= Ri_{cs} + L\frac{di_{cs}}{dt} + e_{cs}
\end{aligned}
\tag{6.1}
$$

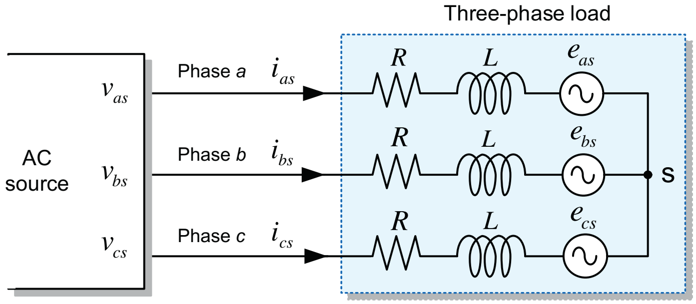

FIGURE 6.7

Three-phase load.

where v_{as}, v_{bs}, v_{cs}, i_{as}, i_{bs}, i_{cs}, and e_{as}, e_{bs}, e_{cs} are three-phase voltages, currents, and back-EMFs, respectively, and R and L are the resistance and inductance of the load, respectively.

Applying the axis transformation described in Chapter 4 we can transform the three-phase voltage equations of Eq. (6.1) into $d-q$ forms in the stationary reference frame as

$$v_{ds}^s = Ri_{ds}^s + L\frac{di_{ds}^s}{dt} + e_{ds}^s \tag{6.2}$$

$$v_{qs}^s = Ri_{qs}^s + L\frac{di_{qs}^s}{dt} + e_{qs}^s \tag{6.3}$$

The current regulator for the d- and q-axes currents in the stationary reference frame based on Eqs. (6.2) and (6.3) is shown in Fig. 6.8.

In this stationary reference frame $d-q$ axes current regulator, the three-phase load currents i_{as}, i_{bs}, i_{cs} should be transformed into the stationary frame $d-q$ currents to be used as feedback currents. The PI control is normally used to regulate these currents to the desired values. The PI regulators produce $d-q$ axes reference voltages v_{ds}^{s*}, v_{qs}^{s*} to eliminate the current errors, and these voltages are transformed into three-phase reference voltages v_{as}^*, v_{bs}^*, v_{cs}^*. A voltage source PWM inverter, which will be discussed in detail in Chapter 7.

Let us evaluate the characteristic of the stationary reference frame $d-q$ current regulator. Fig. 6.9 shows the block diagram of this regulator.

The transfer function of this system is given as

$$I_{dqs}(s) = \frac{K_p s + K_i}{Ls^2 + (R + K_p)s + K_i} I_{dqs}^*(s) - \frac{s}{Ls^2 + (R + K_p)s + K_i} E_{dqs}(s) \tag{6.4}$$

From Eq. (6.4), it can be seen that if the current reference $I_{dqs}^*(s)$ is an AC quantity (i.e., $s \neq 0$), the actual current $I_{dqs}(s)$ never follows its reference $I_{dqs}^*(s)$ unless the current regulator has infinite gains. Thus when AC currents are regulated by the stationary regulator, the amplitude and phase errors will exist in the steady state.

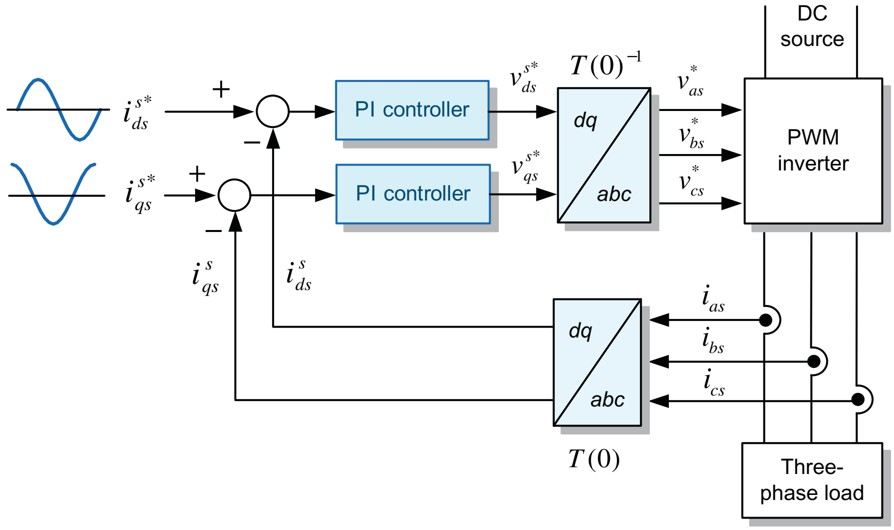

FIGURE 6.8

Stationary reference frame d–q axes current regulator.

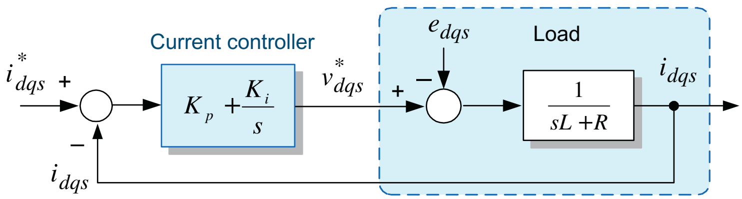

FIGURE 6.9

Block diagram for one axis of a stationary frame current regulator.

On the other hand, if the current reference $I_{dqs}^{*}(s)$ is a DC quantity (i.e., $s = 0$), Eq. (6.4) becomes

$$\frac{I_{dqs}(s)}{I_{dqs}^{*}(s)}\Big|_{s=0} = 1 \tag{6.5}$$

This indicates that the actual current $I_{dqs}(s)$ can follow its reference value $I_{dqs}^{*}(s)$ accurately, i.e., the steady-state error is zero. This fact implies that instead of controlling the load current as an AC quantity directly, it is desirable to control the load current transformed as a DC quantity. For this purpose, the current control needs to be performed in the synchronous reference frame, where the currents of the AC load can be given as DC quantities. This regulator is called the *synchronous reference frame d–q current regulator*, which is widely used for the current control of AC systems.

6.3.2 SYNCHRONOUS REFERENCE FRAME *d-q* CURRENT REGULATOR [2]

Transforming the stationary frame voltage equations of Eqs. (6.2) and (6.3) into the synchronous reference frame, which is rotating at the electrical angular frequency ω_e corresponding to the operating frequency of the three-phase currents, gives

$$v_{ds}^e = Ri_{ds}^e + L\frac{di_{ds}^e}{dt} - \omega_e L i_{qs}^e + e_{ds}^e \tag{6.6}$$

$$v_{qs}^e = Ri_{qs}^e + L\frac{di_{qs}^e}{dt} + \omega_e L i_{ds}^e + e_{qs}^e \tag{6.7}$$

Unlike the stationary reference frame, in these equations, all the electrical variables such as currents, voltages, and back-EMFs are all DC quantities in the steady state. It should be noted that, in addition to the back-EMFs e_{ds}^e and e_{qs}^e, there are $-\omega_e L i_{qs}^e$ and $\omega_e L i_{ds}^e$ (called *speed voltages*) in the synchronous reference frame expressions of Eqs. (6.6) and (6.7). These speed voltages are cross-coupled between *d*- and *q*-axes. Thus a change in the *d*-axis current may affect the control of the *q*-axis current and vice versa. These are the major disturbances on this synchronous current regulator. Thus the feedforward compensation of the speed voltages as well as the back-EMF voltages should be employed to achieve a good current control performance. This will be discussed in detail in a later section.

The block diagram for a current regulator operating on the synchronous reference frame is shown in Fig. 6.10.

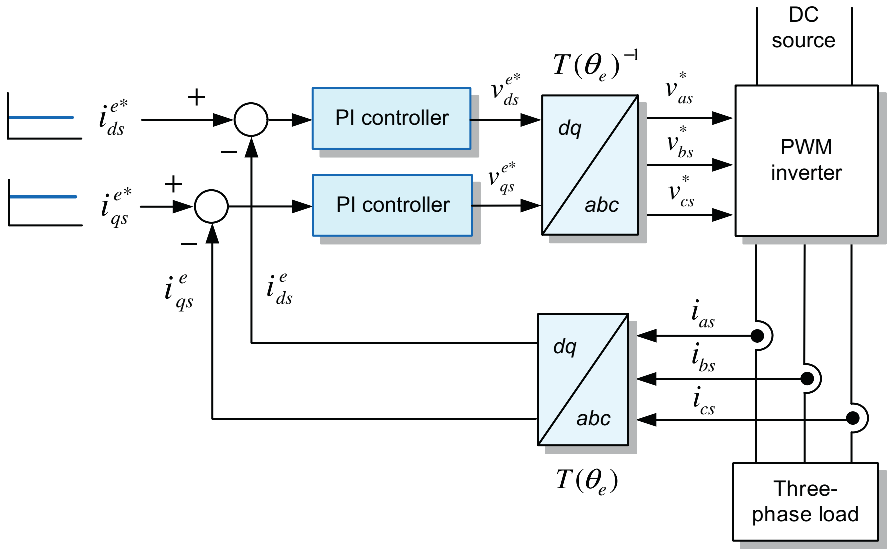

FIGURE 6.10

Block diagram of a synchronous frame current regulator.

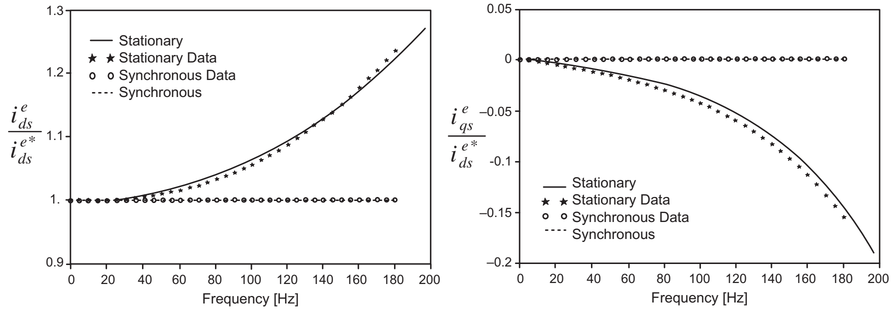

FIGURE 6.11

Comparison between the stationary and the synchronous frame regulators [2].

The structure of this regulator seems to be similar to that of a stationary frame current regulator in Fig. 6.8, but the controlled currents are DC quantities and a different transformation is used in this system. Since the synchronous reference frame uses DC quantities, the currents can be regulated well by using a PI controller.

Fig. 6.11 depicts the performance comparison between the stationary frame and the synchronous frame current regulators in the steady state for $R-L$ load [2]. From the left figure showing the performance of the d-axis current control, it can be seen that the steady-state error for the stationary frame current regulator increases with the operating frequency of the reference current. On the other hand, the synchronous frame current regulator has no steady-state error, regardless of the operating frequency. In addition, we can see that there is a cross-coupling between the axes for the stationary frame current regulator in the right figure. The control error for the q-axis current increases as the operating frequency of the d-axis reference current increases for the stationary frame current regulator.

6.3.3 GAIN SELECTION OF THE SYNCHRONOUS REFERENCE FRAME PI CURRENT REGULATOR

In Chapter 2, we described how to select the PI gains of a current controller for DC motors. Since a synchronous reference frame current regulator also controls DC quantities, we can directly use such method to select the PI gains of a synchronous reference frame current regulator. By referring to the gain selection of the current controller for a DC motor in Section 2.6, we can determine the proportional gain and the integral gain of a synchronous reference frame current regulator for the three-phase AC load as:

$$\text{Proportional gain:} \quad K_p = L \cdot \omega_c \tag{6.8}$$

$$\text{Integral gain:} \quad K_i = R \cdot \omega_c \tag{6.9}$$

where R and L denote the resistance and inductance of the load, respectively, and ω_c denotes the control bandwidth of the current regulator. Here, the proportional gain is determined by the required control bandwidth ω_c of the current regulator, and the integral gain is determined by the relationship of $K_p/K_i = L/R$ (*pole-zero cancellation*).

On the basis of the current control for the three-phase AC load as mentioned earlier, it can readily be seen that it is better to use a synchronous frame current regulator for the current control of AC motors. For this case, the PI gains can be obtained directly from Eqs. (6.8) and (6.9). However, since the resistance and inductance values differ from system to system, we need to find the equivalent R and L values corresponding to the chosen AC motor. The values of these equivalent parameters for induction motors and synchronous motors can be obtained as follows.

6.3.3.1 Proportional–integral gains for induction motors

From Eqs. (4.86) and (4.87), the $d-q$ voltage equations of an induction motor in the synchronous reference frame are given as

$$v_{ds}^e = Ri_{ds}^e + p\lambda_{ds}^e - \omega_e\lambda_{qs}^e \tag{6.10}$$

$$v_{qs}^e = Ri_{qs}^e + p\lambda_{qs}^e + \omega_e\lambda_{ds}^e \tag{6.11}$$

The stator flux linkages in these equations can be expressed as the rotor flux linkages and the stator currents as

$$\begin{aligned}\lambda_{ds}^e &= L_s i_{ds}^e + L_m i_{dr}^e \\ &= L_s i_{ds}^e + L_m\left(\frac{\lambda_{dr}^e - L_m i_{ds}^e}{L_r}\right) = \sigma L_s i_{ds}^e + \frac{L_m}{L_r}\lambda_{dr}^e\end{aligned} \tag{6.12}$$

$$\begin{aligned}\lambda_{qs}^e &= L_s i_{qs}^e + L_m i_{qr}^e \\ &= L_s i_{qs}^e + L_m\left(\frac{\lambda_{qr}^e - L_m i_{qs}^e}{L_r}\right) = \sigma L_s i_{qs}^e + \frac{L_m}{L_r}\lambda_{qr}^e\end{aligned} \tag{6.13}$$

where $\sigma = 1 - L_m^2/L_sL_r$ and the rotor currents can be obtained from the rotor flux linkages as

$$i_{dr}^e = \frac{\lambda_{dr}^e - L_m i_{ds}^e}{L_r} \leftarrow \lambda_{dr}^e = L_r i_{dr}^e + L_m i_{ds}^e \tag{6.14}$$

$$i_{qr}^e = \frac{\lambda_{qr}^e - L_m i_{qs}^e}{L_r} \leftarrow \lambda_{qr}^e = L_r i_{qr}^e + L_m i_{qs}^e \tag{6.15}$$

Substituting Eqs. (6.12) and (6.13) into Eqs. (6.10) and (6.11) gives

$$\begin{aligned} v_{ds}^e &= R_s i_{ds}^e + p\lambda_{ds}^e - \omega_e \lambda_{qs}^e \\ &= R_s i_{ds}^e + p\left(\sigma L_s i_{ds}^e + \frac{L_m}{L_r}\lambda_{dr}^e\right) - \omega_e\left(\sigma L_s i_{qs}^e + \frac{L_m}{L_r}\lambda_{qr}^e\right) \\ &= \left(R_s + R_r\frac{L_m^2}{L_r^2}\right) i_{ds}^e + \sigma L_s \frac{di_{ds}^e}{dt} - \omega_e \sigma L_s i_{qs}^e - R_r \frac{L_m}{L_r^2}\lambda_{dr}^e - \omega_r \frac{L_m}{L_r}\lambda_{qr}^e \end{aligned} \tag{6.16}$$

$$\begin{aligned} v_{qs}^e &= R_s i_{qs}^e + p\lambda_{qs}^e + \omega_e \lambda_{ds}^e \\ &= R_s i_{qs}^e + p\left(\sigma L_s i_{qs}^e + \frac{L_m}{L_r}\lambda_{qr}^e\right) + \omega_e\left(\sigma L_s i_{ds}^e + \frac{L_m}{L_r}\lambda_{dr}^e\right) \\ &= \left(R_s + R_r\frac{L_m^2}{L_r^2}\right) i_{qs}^e + \sigma L_s \frac{di_{qs}^e}{dt} + \omega_e \sigma L_s i_{ds}^e - R_r \frac{L_m}{L_r^2}\lambda_{qr}^e + \omega_r \frac{L_m}{L_r}\lambda_{dr}^e \end{aligned} \tag{6.17}$$

In the vector control, since $\lambda_{qr}^e = 0$, the above equations will be reduced as

$$v_{ds}^e = \left(R_s + R_r\frac{L_m^2}{L_r^2}\right) i_{ds}^e + \sigma L_s \frac{di_{ds}^e}{dt} - \omega_e \sigma L_s i_{qs}^e - R_r \frac{L_m}{L_r^2}\lambda_{dr}^e \tag{6.18}$$

$$v_{qs}^e = \left(R_s + R_r\frac{L_m^2}{L_r^2}\right) i_{qs}^e + \sigma L_s \frac{di_{qs}^e}{dt} + \omega_e \sigma L_s i_{ds}^e + \omega_r \frac{L_m}{L_r}\lambda_{dr}^e \tag{6.19}$$

From these, the equivalent R and L values of induction motors are given as

$$R = R_s + R_r\left(\frac{L_m}{L_r}\right)^2 \tag{6.20}$$

$$L = \sigma L_s \tag{6.21}$$

Thus the PI gains of a synchronous reference frame current regulator for induction motors are given as

$$\text{Proportional gain:} \quad K_p = \sigma L_s \cdot \omega_c \tag{6.22}$$

$$\text{Integral gain:} \quad K_i = \left[R_s + R_r\left(\frac{L_m}{L_r}\right)^2\right]\cdot \omega_c \tag{6.23}$$

6.3.3.2 Proportional–integral gains for permanent magnet synchronous motors

From Eqs. (4.106), (4.107), (4.113), and (4.114), the $d-q$ voltage equations of a permanent magnet synchronous motor (PMSM) in the synchronous reference frame rotating at the angular frequency ω_r of the rotor are given as

$$v_{ds}^r = R_s i_{ds}^r + L_{ds}\frac{di_{ds}^r}{dt} - \omega_r L_{qs} i_{qs}^r \tag{6.24}$$

$$v_{qs}^r = R_s i_{qs}^r + L_{qs}\frac{di_{qs}^r}{dt} + \omega_r (L_{ds} i_{ds}^r + \phi_f) \tag{6.25}$$

From these, it can be seen that the equivalent R value of a PMSM for the synchronous frame current regulator is the stator resistance R_s, and the equivalent L value is the stator inductance. For a surface-mounted PMSM, the d- and q-axes inductances have the same value. However, since they are different for an interior PMSM, the equivalent L value according to the axis is different as the following.

$$R = R_s \tag{6.26}$$

$$L = L_{ds} \quad (d\text{-axis}), \quad L = L_{qs} \quad (q\text{-axis}) \tag{6.27}$$

Thus the PI gains of the synchronous frame current regulator for a PMSM are given as

$$\text{Proportional gain:} \quad K_{pd} = L_{ds} \cdot \omega_c, \quad K_{pq} = L_{qs} \cdot \omega_c \tag{6.28}$$

$$\text{Integral gain:} \quad K_i = R_s \cdot \omega_c \tag{6.29}$$

6.4 FEEDFORWARD CONTROL

As described in the Section 6.3.2, a synchronous frame PI current regulator has been widely used for the current control for AC systems because it can achieve zero steady-state error and provide a good transient performance in spite of its simple structure. We saw in Section 6.3.2 that the voltage expressions of an AC system in the synchronous reference frame have cross-coupling components, $-\omega_e L i_{qs}^e$ and $\omega_e L i_{ds}^e$, between the axes in addition to back-EMF as

$$v_{ds}^e = R i_{ds}^e + L\frac{di_{ds}^e}{dt} - \omega L i_{qs}^e + e_{ds}^e \tag{6.30}$$

$$v_{qs}^e = R i_{qs}^e + L\frac{di_{qs}^e}{dt} + \omega L i_{ds}^e + e_{qs}^e \tag{6.31}$$

These are described as a block diagram in Fig. 6.12.

These voltage components can have a negative influence on the feedback current control although a synchronous frame current regulator is used. In particular, at high operating frequencies where they become large, these components can incur an oscillatory current response. If the bandwidth of the current controller is large enough, then their influence can be reduced. However, as explained in Section 2.6.1.1, the value of the gains is limited by the switching frequency and the current sampling frequency. Moreover, large gains make the system more sensitive to noise. To eliminate the effect of these disturbance components and improve the performance of the current control, the *feedforward control*

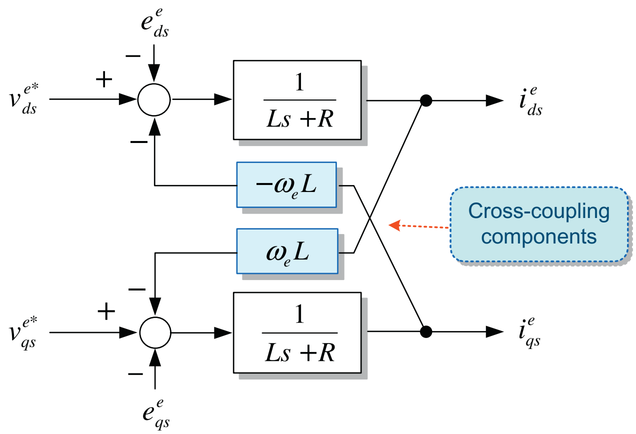

FIGURE 6.12

Voltage expressions in the synchronous frame.

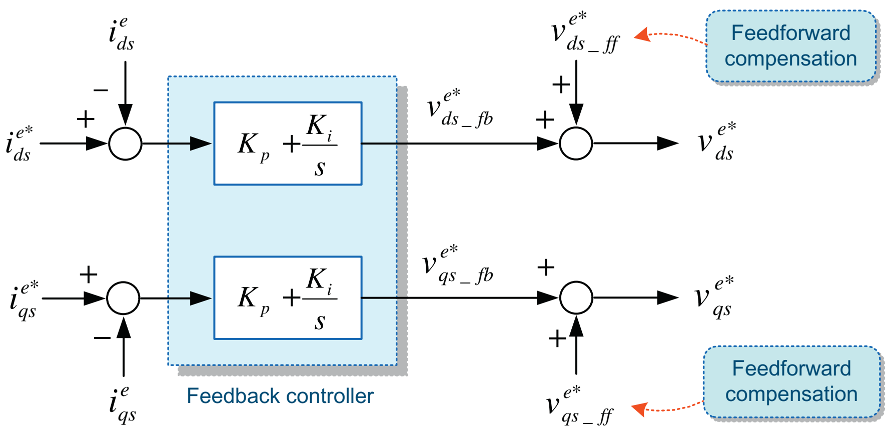

FIGURE 6.13

Current regulator with the feedforward control.

(also called the *decoupling control*), described in Section 2.5, is usually used along with the feedback control [4].

Fig. 6.13 shows a synchronous frame current regulator with the feedforward control for decoupling the cross-coupling.

When using the feedforward control, the output voltage of the synchronous frame current regulator consists of two components as follows:

$$v_{ds}^{e*} = v_{ds\_fb}^{e*} + v_{ds\_ff}^{e*} \tag{6.32}$$

$$v_{qs}^{e*} = v_{qs\_fb}^{e*} + v_{qs\_ff}^{e*} \tag{6.33}$$

where $v^{e*}_{ds\_fb}, v^{e*}_{qs\_fb}$ are the feedback voltage components produced by the PI current controller and $v^{e*}_{ds\_ff}, v^{e*}_{qs\_ff}$ are the feedforward voltage components. From Eqs. (6.30) and (6.31), the $d-q$ axes feedforward components for a three-phase $R-L$ load are given as

$$v^{e*}_{ds\_ff} = -\omega_e L i^e_{qs} + e^e_{ds} \tag{6.34}$$

$$v^{e*}_{qs\_ff} = \omega_e L i^e_{ds} + e^e_{qs} \tag{6.35}$$

In the current control of AC motors, the feedforward components vary depending on the motor. The feedforward components for an induction motor and a PMSM can be obtained as follows.

6.4.1 FEEDFORWARD CONTROL FOR INDUCTION MOTORS

To identify the feedforward voltage components for an induction motor, Eqs. (6.18) and (6.19) are rewritten as

$$v^e_{ds} = \left(R_s + R_r \frac{L_m^2}{L_r^2}\right) i^e_{ds} + \sigma L_s \frac{di^e_{ds}}{dt} \underline{- \omega_e \sigma L_s i^e_{qs} - R_r \frac{L_m}{L_r^2} \lambda^e_{dr}} \tag{6.36}$$

$$v^e_{qs} = \left(R_s + R_r \frac{L_m^2}{L_r^2}\right) i^e_{qs} + \sigma L_s \frac{di^e_{qs}}{dt} \underline{+ \omega_e \sigma L_s i^e_{ds} + \omega_r \frac{L_m}{L_r} \lambda^e_{dr}} \tag{6.37}$$

Here, the third and the fourth underlined terms on the right-hand side express the feedforward voltage components. Thus

$$v^e_{ds\_ff} = -\omega_e \sigma L_s i^e_{qs} - R_r \frac{L_m}{L_r^2} \lambda^e_{dr} \tag{6.38}$$

$$v^e_{qs\_ff} = \omega_e \sigma L_s i^e_{ds} + \omega_r \frac{L_m}{L_r} \lambda^e_{dr} \tag{6.39}$$

6.4.2 FEEDFORWARD CONTROL FOR PERMANENT MAGNET SYNCHRONOUS MOTORS

To identify the feedforward voltage components for an PMSM, Eqs. (6.24) and (6.25) are rewritten as

$$v^r_{ds} = R_s i^r_{ds} + L_{ds} \frac{di^r_{ds}}{dt} \underline{- \omega_r L_{ds} i^r_{qs}} \tag{6.40}$$

$$v^r_{qs} = R_s i^r_{qs} + L_{qs} \frac{di^r_{qs}}{dt} \underline{+ \omega_r L_{ds} i^r_{ds} + \omega_r \phi_f} \tag{6.41}$$

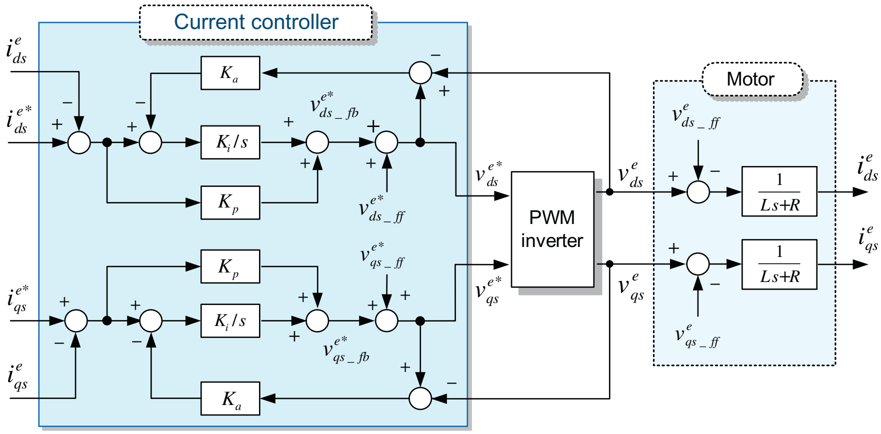

FIGURE 6.14

Synchronous frame PI current regulator with the feedforward control. *PI*, proportional–integral.

Here, the third and the fourth underlined term on the right-hand side express the feedforward voltage components. Thus

$$v_{ds\_ff}^{r*} = -\omega_r L_{qs} i_{qs}^{r} \tag{6.42}$$

$$v_{qs\_ff}^{r*} = \omega_r L_{ds} i_{ds}^{r} + \omega_r \phi_f \tag{6.43}$$

By using such feedforward control, the motor can be simplified to an $R-L$ passive circuit, so an improved current control performance can be achieved. An accurate feedforward compensation requires an accurate knowledge of inductances, flux linkage, and speed. Even when there are errors in these quantities, the feedforward control can largely reduce the effect of the disturbances by back-EMFs and cross-coupling components on the current control when compared with the feedback control alone.

In the feedforward control, it is desirable to estimate the feedforward voltage components by using the measured currents. Such feedforward control that uses measured currents for estimation is called *state feedback decoupling control*.

Fig. 6.14 shows a synchronous frame PI current regulator with the feedforward control, which has become the industry standard for the high-performance current control of AC motors. A PI current regulator needs to include an anti-windup controller to prevent integrator saturation, which was described in detail in Section 2.6.2.

6.5 COMPLEX VECTOR CURRENT REGULATOR

An ideal synchronous reference frame current regulator has a time response independent of the operating frequency. However, in reality, its transient performance degrades as the operating frequency approaches the bandwidth of the current regulator.

In the design of a PI current controller, as described in Chapter 2, the zero of the PI controller is made equal to the pole of the plant for pole-zero cancellation, i.e., $K_p/K_i = L/R$. At low operating frequencies, the controller zero can cancel the plant pole relatively completely. This allows a faster response of the system corresponding to the given control bandwidth. However, as the operating frequency increases, the plant pole and the controller zero move apart, resulting in a degradation of the system performance. The decoupling control as mentioned in Section 6.4 can make the performance of the current regulator to be independent of the operating frequency, i.e., the plant pole to be independent of the operating frequency.

A synchronous frame current regulator with the state feedback decoupling control is shown in Fig. 6.15. An accurate decoupling control requires the correct knowledge of system parameters (here, the inductance value). If the system parameters are incorrect, then the estimated value of the feedforward compensation becomes inaccurate, so the controller cannot cancel the plant pole completely. To solve this problem, a complex vector synchronous frame current regulator was proposed [5−7]. In this strategy, by using a complex vector notation, the two-input/two-output system of the synchronous frame $d-q$ current regulator is simplified to an equivalent single-input/single-output complex vector system. Because a complex vector notation is used for the analysis and design of current regulators for multiphase AC loads, this current regulator is called the *complex vector synchronous frame current regulator*.

In contrast to a current regulator with the state feedback decoupling control, a complex vector synchronous frame current regulator has decoupling control inside the PI controller without using any system parameter as shown in Fig. 6.16.

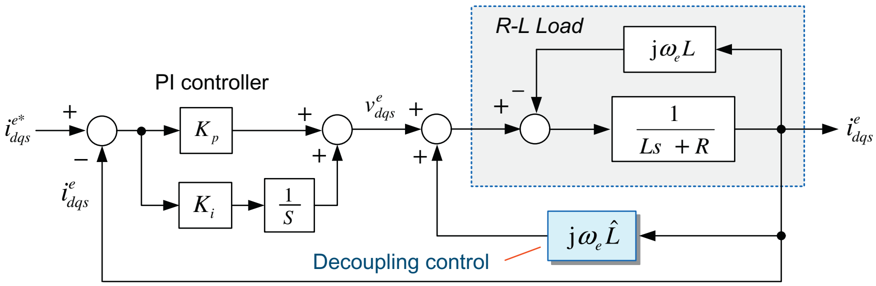

FIGURE 6.15

Synchronous current regulator with the state feedback decoupling control.

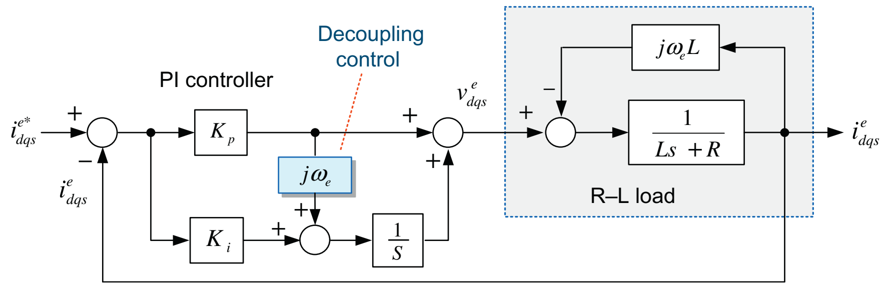

FIGURE 6.16

Complex vector synchronous frame current regulator.

Thus its performance is less sensitive to errors in system parameters, i.e., inductances, and is independent of the operating frequency. However, its response may be slightly oscillatory. If the system parameters used for decoupling control are identical to the actual system parameters, then the performances of these two current regulators are identical.

REFERENCES

[1] D.M. Brod, D.W. Novotny, Current control of VSI-PWM inverters, IEEE Trans. Ind. Appl. IA-21 (4) (1985) 562–570.

[2] T.M. Rowan, R.J. Kerkman, A new synchronous current regulator and an analysis of current-regulated PWM inverter, IEEE Trans. Ind. Appl. IA-22 (4) (1986) 678–690.

[3] M.P. Kazmierkowski, L. Malesani, Current control techniques for three-phase voltage-source PWM converters: a survey, IEEE Trans. Ind. Electron. 45 (5) (1998) 691–703.

[4] F. Briz, M.W. Degner, R.D. Lorenz, Performance of feedforward current regulators for field-oriented induction machine controllers, IEEE Trans. Ind. Appl. IA-23 (4) (1987) 597–602.

[5] F. Briz, M.W. Degner, R.D. Lorenz, Analysis and design of current regulators using complex vectors, in: Conference Record of the IEEE-IAS Annual Meeting, 1997, pp. 1504–1511.

[6] F. Briz, M.W. Degner, R.D. Lorenz, Dynamic analysis of current regulators for AC motors using complex vectors, IEEE Trans. Ind. Appl. 35 (6) (1999) 1424–1432.

[7] H. Kim, R.D. Lorenz, Analysis and design of current regulators using complex vectors, in: Conference Record of the IEEE-IAS Annual Meeting, 2004, pp. 856–863.